Journal of Nuclear Materials 404 (2010) 116–120

Contents lists available at ScienceDirect

Journal of Nuclear Materials

journal homepage: www.elsevier.com/locate/jnucmat

Elastic and thermodynamic properties of *fcc*-$^6Li_2O$ under high temperatures and pressures ☆

Ren Weiyi [a], Wang Feng [b,*], Zheng Zhou [c], Xu Pingchuan [a], Sun Weiguo [d]

[a] Institute of Theoretical Physics, China West Normal University, Nanchong 637002, China
[b] School of Science, Chongqing Jiaotong University, Chongqing 400074, China
[c] Institute of Nuclear Physics and Chemistry, CAEP, Mianyang 621900, China
[d] Institute of Atomic and Molecular of Sichuan University, Chengdu 610065, China

ARTICLE INFO

Article history:
Received 2 April 2010
Accepted 28 June 2010

ABSTRACT

The elastic and thermodynamic properties of *fcc*-$^6Li_2O$ under high temperatures and pressures are investigated using the Density functional theory and quasi-harmonic Debye model. Calculation indicates that the lattice constant of $^6Li_2O$ at ground state is a little larger than that of $^7Li_2O$. Pressure can suppress thermal expansion effectively. When it is 1200 K, just only 8.59 GPa can pressure restrain the volume expansion caused by temperature. Elastic constants illuminate that crystal lattice of $^6Li_2O$ is mechanical stable under high temperature and temperature. Compared with $^7Li_2O$, shear of $^6Li_2O$ on the {1 0 0} and {1 1 0} planes caused by high pressure and temperature is lower. Heat capacity of different pressure increases with temperature and closes to the Dulong–Petit limit at higher temperatures. Debye temperature decreases with temperature, and increases with pressure. Under lower pressure, thermal expansion coefficient raise rapidly with temperature, and then the increasing trend will get slow at higher pressure and temperature.

1. Introduction

fcc-$^6Li_2O$ may be one of the most important solid breeder materials for future use in magnetic or inertial-confinement fusion reactors because of its uniquely high lithium atom density coupled with a high melting point and relatively low volatility. The lithium atom density in *fcc*-$^6Li_2O$ (about 0.88 g $^6Li/cm^3$ at 1000 K) exceeds that in the pure metal by a factor of 2 and that in γ-$LiAlO_2$, the leading contender as a solid breeder, by a factor of 3. Furthermore, Li_2O has attracted considerable interest over the years, among others for being a superionic conductor with a potential for use in the construction of solid state batteries [1].

When a fast neutron incident on a *fcc*-$^6Li_2O$ lattice, the α and ^3H are absorbed in the crystal ($^6Li + {}^1n \rightarrow {}^3H + {}^4\alpha + \Delta$) [2], resulting in an obvious temperature and pressure rise which will cause crystal lattice damage. Demontis et al. [3,4] have predicted that a further transformation to an antifluorite phase in ice at some pressure above 150 GPa, and experiments show changes in vibrational mode coupling [5] and single-crystal X-ray diffraction peak intensity [6] near 150 GPa. In further similarity to ice, for which a high pressure, high temperature superionic phase has been predicted [7], ambient pressure Li_2O becomes superionic at temperatures above 1350 K [8], prior to melting at 1705 K [9]. Then, understanding the behavior of $^6Li_2O$ at high temperatures and pressures is, therefore, very useful for its applications as well as a potential aid in understanding the behavior of the hot, dense structures which are of such great importance to planetary science, geosciences, and fundamental chemistry. Additionally, investigation of this simple material is a reference point for understanding more complex metal-oxides.

Unfortunately, because the measurement of thermodynamic properties of $^6Li_2O$ under high temperatures and pressures is very difficult and $^6Li_2O$ is quite rare and expensive, to our knowledge, detailed thermodynamic properties data for $^6Li_2O$ at different temperatures and pressures are not available from experimental methods. Therefore, we need acquiring these data by theoretical methods. In our work, structure, elastic properties, heat capacity and thermal expansion, etc. of $^6Li_2O$ are studied in detail by Density functional theory and quasi-harmonic Debye model. The results obtained in this work may be useful for other groups working on or with $^6Li_2O$.

2. Theoretical method

It is well known that the elastic constants are calculated by means of Taylor expansion of the total energy, $E(V, \delta)$, for the

☆ This work is supported by the Sichuan province Educational Technological Office, China (Grant No. 009JY0143) and the Science Foundation of Sichuan province Educational Bureau, China (Grant No. 09ZA124).

* Corresponding author.
E-mail address: wfbgc@yahoo.com.cn (W. Feng).

0022-3115/$ - see front matter Crown Copyright © 2010 Published by Elsevier B.V. All rights reserved.
doi:10.1016/j.jnucmat.2010.06.035

system with respect to a small strain δ of the cell volume V. The elastic energy of a strained system is expressed as follows [10]:

$$E(V,\delta) = E(V_0,0) + V_0\left(\sum_i \tau_i\delta_i\xi_i + \frac{1}{2}\sum_{ij} C_{ij}\delta_i\xi_i\delta_j\xi_j\right) \quad (1)$$

where $E(V_0, 0)$ is the energy of the unstrained system with equilibrium volume V_0, τ_i is an element of stress tensor, and ξ_i is a factor present to take care of the Voigt index [10]. There are three independent components of the elastic tensor for *fcc*-$^6Li_2O$, i.e. C_{11}, C_{12}, and C_{44}. C_{11} is obtained directly by deforming one of the three edges of the cubic unit cell. C_{12} is given indirectly, via the linear combination $C_{11}-C_{12}$, from a volume-conserving strain involving the contraction of the two edges and the stretching of the other by twice as much. The shear constant C_{44} resulted from the application of a volume-conserving rhombohedral strain along the $\langle 1\,1\,1\rangle$ direction. A detailed description of the calculation method has been reported in Ref. [11]. In our calculations, the strains enforced in the crystal are labeled in Table 1. Without considering the phononic effect in *fcc*-$^6Li_2O$, we obtain the elastic constants and the bulk modulus at different pressure and temperature.

As to thermodynamic properties of $^6Li_2O$ for high temperatures and pressure, we employ Density functional theory (DFT) and quasi-harmonic Debye model [12]. By the methods, thermodynamic properties of ZrH_2 [13], AlFe [14], etc., has been successfully investigated. According to quasi-harmonic Debye model, the thermodynamic properties of crystal can be obtained by the function of $E(V)$ (total crystal energy at different cell volume) [12].

In order to obtain $E(V)$, lattice parameter (a), bulk modulus (B) and the elastic constants (C_{ij}) etc., CASTEP code [15,16] is employed. We here use the non-local ultrasoft pseudopotential, together with the Perdew–Burke–Ernzerhof (PBE) generalized gradient approximation (GGA) exchange–correlation function [15,16]. A plane wave basis set with energy cut-off 380.00 eV is applied. Pseudo atomic calculations are performed for ^{6}Li $1s^22s^1$, O $2s^22p^4$. For the Brillouin-zone sampling, we use the $6\times6\times6$ Monkhorst–Pack mesh, where the self-consistent convergence of the total energy is at 10^{-6} eV/Atom.

To investigate the thermodynamic properties of $^6Li_2O$, we apply the quasi-harmonic Debye model [12], in which the non-equilibrium Gibbs function $G^*(V;P,T)$ can be written in the form of

$$G^*(V;P,T) = E(V) + PV + A_{vib}[\theta(V);T] \quad (2)$$

where $E(V)$ is the total energy per unit cell, P corresponds to the constant hydrostatic pressure, $\theta(V)$ is the Debye temperature, and A_{vib} is the vibrational Helmholtz free energy, which includes both the vibrational contribution to the internal energy, which can be written, using the Debye model of the phonon density of states, as [17,18]

$$A_{vib}(\theta;T) = nkT\left[\frac{9\theta}{8T} + 3\ln\left(1-e^{-\theta/T}\right) - D\left(\frac{\theta}{T}\right)\right] \quad (3)$$

where n is the number of atoms per formula unit, $D(\theta/T)$ represents the Debye integral, and for an isotropic solid, θ is expressed as [18].

$$\theta = \frac{\hbar}{k}\left[6\pi^2V^{1/2}n\right]^{1/3} f(\sigma)\sqrt{\frac{B_s}{M}} \quad (4)$$

Table 1
The strains used to calculate the elastic constants of *fcc*-$^6Li_2O$.

Strains	Distortion	$\frac{1}{V}\frac{\partial^2E(V,\delta)}{\partial\delta^2}\Big\vert_{\delta=0}$
1	$\varepsilon_{11} = \delta$	C_{11}–P
2	$\varepsilon_{11} = -\varepsilon_{12} = \delta$	$2(C_{11}$–C_{12}–$P)$
3	$\varepsilon_{ij} = \delta\ (i \neq j)$	$4C_{44}$–$2P$

where M is the molecular mass per unit cell (here, atomic mass of ^{6}Li is 6.01512, O is 15.999); B_s is the adiabatic bulk modulus, which is approximated given by the static compressibility [17]. $f(\sigma)$ is given by Eq. (6) [18,19]

$$B_s \cong B(V) = V\frac{d^2E(V)}{dV^2} \quad (5)$$

$$f(\sigma) = \left\{3\left[2\left(\frac{2}{3}\frac{1+\sigma}{1-2\sigma}\right)^{3/2} + \left(\frac{1}{3}\frac{1+\sigma}{1-\sigma}\right)^{3/2}\right]^{-1}\right\}^{1/3} \quad (6)$$

According to Ref. [20], the Poisson σ is taken as 0.25. Therefore, the non-equilibrium Gibbs function G^* as a function of $(V;P,T)$ can be minimized with respect to volume V

$$\left[\frac{\partial G^*(V;P,T)}{\partial V}\right]_{P,T} = 0 \quad (7)$$

By solving Eq. (7), one can obtain the thermal equation-of-state (EOS) $V(P,T)$. The heat capacity C_v and the thermal expansion coefficient α are given by [21]

$$C_v = 3nk\left[4D\left(\frac{\theta}{T}\right) - \frac{3\theta/T}{e^{\theta/T}-1}\right] \quad (8)$$

$$\alpha = \frac{\gamma C_v}{B_T V} \quad (9)$$

where γ is Grüneisen parameter, which is defined as

$$\gamma = -\frac{d\ln\theta(V)}{d\ln V} \quad (10)$$

The E–V, obtained by DFT, is fitted by the Murnaghan equation-of-state [22] to obtain the equilibrium lattice constant under different temperature and pressure. Through the quasi-harmonic Debye model, one could calculate the thermodynamic quantities of $^6Li_2O$ under any temperatures and pressures from the calculated E–V data. To obtain the elastic constants of $^6Li_2O$ we use a numerical DFT calculations by computing the components of the stress tensor ε for small strains. In present work, the elastic and thermodynamic properties of $^6Li_2O$ are determined in the temperature range from 0 to 1200 K and in the pressure from 0 to 120 GPa, where the DFT and quasi-harmonic model remain fully valid.

3. Results and discussion

The results of lattice constant a_0, bulk modulus B_0, and the elastic constants parameters of $^6Li_2O$ under 0 K and 0 GPa are summarized in Table 2, together with some theoretical results and the available experimental data [23–26]. Our calculated lattice parameter and bulk modulus are $a_0 = 4.718$ Å, and $B_0 = 68.081$ GPa. We consider that the number of neutrons in ^{6}Li and ^{7}Li is different, which results in crystal constant is a little larger than the result of other works. According to Johansson and Rosengren [27], the difference of crystal constant between ^{6}Li and ^{7}Li is due to the difference in their nuclear zero-point energy. The change caused by different nuclear mass is more obvious for lighter elements. And, experimentally, it has been observed that ^{6}Li has a larger lattice parameter than ^{7}Li. The relative change is measured to be $\Delta a/a = 0.04\%$ [28]. To the best of our knowledge, there are no detailed experimental works exploring the elastic constants, and no calculations based on the DFT calculations are performed for $^6Li_2O$.

Fig. 1 shows the $(V-V_0)/V_0$ as a function of pressure P and temperature T, where V_0 is the cell volume at $P = 0$, $T = 0$. When $(V-V_0)/V_0 > 0$, crystal lattice is being expanded, $(V-V_0)/V_0 < 0$ means being compressed. The absolute values of $(V-V_0)/V_0$ express the volume variation of the crystal cell. It is well known,

Table 2
Lattice constant a_0, bulk modulus B_0, and the elastic constants parameters of $^6Li_2O$ at zero pressure and zero temperature.

	Present work of $^6Li_2O$	Experimental and other results of Li_2O
a_0 (Å)	4.718	4.573[a], 4.533[b], 4.607[c], 4.573[d]
B_0 (GPa)	68.081	92.6[a], 89.0[b], 80.0[c], 88.0[d]
C_{11} (GPa)	182.734	233.7[a], 238.0[b], 202.0[c], 217 ± 4[d]
C_{12} (GPa)	10.754	22.1[a], 16.0[b], 19.0[c], 25 ± 6[d]
C_{44} (GPa)	49.144	67.5[a], 66.0[b], 59.0[c], 68 ± 1[d]

[a] Ref. [23].
[b] Ref. [24].
[c] Ref. [25].
[d] Ref. [26].

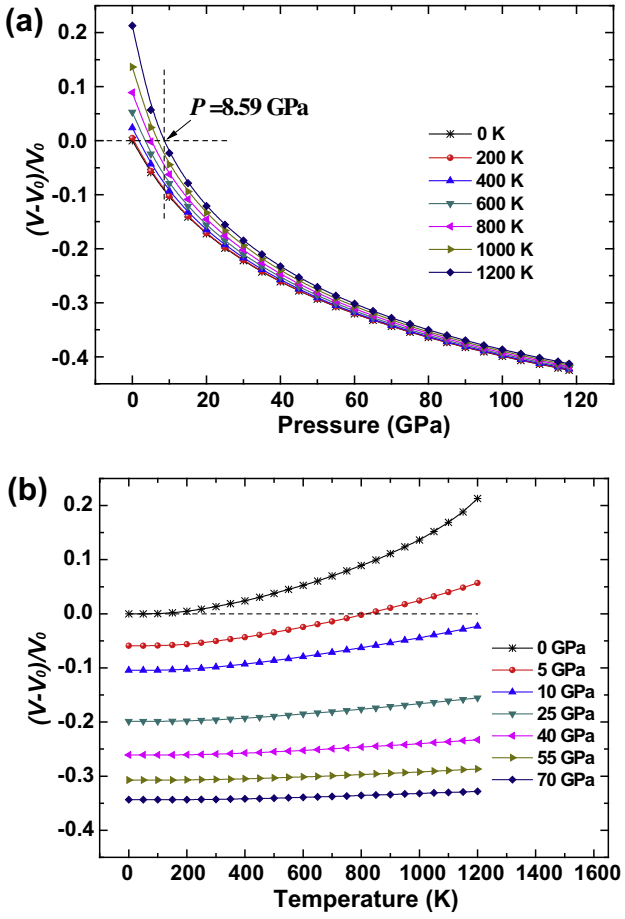

Fig. 1. The $(V - V_0)/V_0$ as a function of pressure P and temperature T, V_0 is the cell volume at $P = 0$, $T = 0$. (a): $(V - V_0)/V_0$–P curves; (b): $(V - V_0)/V_0$–T curves.

the effects to cell volume caused by temperature and pressure are reversed. Temperature causes expansion, pressure induces compression. In present work, volume variation is more sensitive to pressure. For instance, when temperature is 1200 K, just 8.59 GPa can pressure restrain the volume expansion caused by temperature, cell volume keep to V_0 (Fig. 1a). As shown in Fig. 1a, the crystal cell is being compressed under any temperature (0–1200 K), when $P > 8.59$ GPa. And the lower the temperature is, the larger the degree of compression is. However, with increasing pressure, the volume variations of different temperature close together gradually, which indicates that, under higher pressure, temperature effect to cell volume is no longer obvious. The phenomenon is quite different to which of *fcc*-^{6}LiF [29]. The Fig. 1b shows that crystal lattice expands obviously at high temperature without pressure or under low pressure. However, thermal expansion of lattice is quite tiny under high pressures, which means that thermal expansion is suppressed by pressure. The results is absolutely consistent with Fig. 1a.

Crystal constant a, bulk modulus B, and the elastic constants of $^6Li_2O$ under different pressure and temperature obtained are listed in Table 3. As shown in Table 3, crystal constant decreases with pressure and increases with temperature, which is agree with the results of Fig. 1. We also found that B rises with pressure and reduces with temperature. According to C. Kittel [30], $B = 1/K$ (K is compressibility), which indicates that compressibility of $^6Li_2O$ is lower at high pressure (temperature is 0 K), but larger at high temperature (pressure is 0 GPa).

Unfortunately, there are no detailed experimental data of $^6Li_2O$ for checking our calculated elastic constants under different pressure and temperature. The mechanical stability in a cubic crystal under isotropic pressure is judged using the following condition [11]:

$$\tilde{C}_{44} > 0, \quad \tilde{C}_{11} - |\tilde{C}_{12}| > 0, \quad \tilde{C}_{11} + 2\tilde{C}_{12} > 0 \tag{11}$$

where $\tilde{C}_{\alpha\alpha} = C_{\alpha\alpha} - P$, $\tilde{C}_{12} = C_{12} + P$. It is obvious from Table 3 that C_{11}, C_{12}, C_{44} and B increase monotonically with increasing pressure. Except $T = 0$ K, $P = 118$ GPa, the elastic constants under pressures and temperatures are consistent with Eq. (11), indicating that $^6Li_2O$ should be stable when pressure is less than 118 GPa. It means that crystal lattice will be destroyed under too high pressure. For cubic crystals, with elastic constants C_{11}, C_{12} and C_{44}, there are two shear moduli, c and c' corresponding to shear on the {1 0 0} and {1 1 0} planes respectively [20]:

$$c = C_{44}$$

$$c' = \frac{1}{2}(C_{11} - C_{12})$$

Fig. 2 shows c and c' of $^6Li_2O$ compared with other data of Li_2O [31] at different temperature and pressure. As shown in Fig. 2a, c and c' of $^6Li_2O$ increase slowly with pressure. Which indicates that, when temperature is 0 K, increasing of shears on the {1 0 0} and {1 1 0} planes are not obvious under high pressure. It is found that c and c' of $^7Li_2O$ [31] rise with pressure distinctly ($T = 0$ K), and they are greatly more than those of $^6Li_2O$, which indicate that the crystal lattice of $^7Li_2O$ can be sheared easily. Compared with the data of $^7Li_2O$, c and c' of $^6Li_2O$ are more steady under high pressure. When pressure is 0 GPa, c, c' of $^6Li_2O$ and $^7Li_2O$ are listed in Fig. 2b. With increasing temperature, c, c' of $^6Li_2O$ and $^7Li_2O$ reduce gradually. The c of $^6Li_2O$ and Li_2O [8,31–32] are mainly consistent with each other. Though the downtrends of c' of $^6Li_2O$ and Li_2O are alike, the value of $^7Li_2O$ is more than that of $^6Li_2O$. Fig. 2b illuminates that shears on the {1 0 0} and {1 1 0} planes of $^6Li_2O$ and $^7Li_2O$ decrease with temperature tardily, which means that high temperature will not cause sharp variation of shear on the {1 0 0} and {1 1 0} planes.

Figs. 3 and 4 represent the heat capacity $C_v(T)$, and Debye temperature $\theta(T)$ as function of the temperature, respectively. $C_v(T)$ and $\theta(T)$ of $^6Li_2O$ are quite significant. The investigation on the heat capacity of crystals is an old topic of the condensed matter physics [33–35]. Knowledge of the heat capacity of a substance not only provides essential insight into its vibrational properties but is also mandatory for many applications. The Debye temperature is closely related to many physical properties of solids, such as elastic constants, specific heat, and melting temperature. At low temperatures the vibrational excitations arise solely from acoustic vibrations. Two famous limiting cases are correctly predicted by the standard elastic continuum theory [35]. At high temperatures, the constant-volume heat capacity C_v tends to the Petit and Dulong limit [36]. At sufficiently low temperatures, C_v is proportional to T^3 [35]. At intermediate temperatures, however, the temperature

Table 3
Lattice constant a, bulk modulus B, and the elastic constants parameters of $^6Li_2O$ at different temperature and pressure.

$T = 0$ P (GPa)	a (Å)	B (GPa)	C_{11} (GPa)	C_{12} (GPa)	C_{44} (GPa)	$\tilde{C}_{44}$	$\tilde{C}_{11} - \lvert\tilde{C}_{12}\rvert$	$\tilde{C}_{11} + 2\lvert\tilde{C}_{12}\rvert$
0.000	4.718	68.081	182.734	10.754	49.144	49.144	171.981	204.242
15.000	4.484	121.544	252.067	56.283	79.396	64.396	165.785	379.632
30.000	4.339	169.945	309.945	99.945	97.553	67.553	149.999	539.835
45.000	4.233	217.252	363.603	110.131	144.076	99.076	163.472	628.865
60.000	4.148	263.405	413.700	188.258	119.037	59.037	105.443	850.216
75.000	4.078	307.852	461.145	231.206	126.271	51.271	79.939	998.556
90.000	4.017	351.539	506.654	273.981	130.087	40.087	52.673	1144.616
105.000	3.965	396.966	554.508	318.195	134.986	29.986	26.313	1295.898
118.000	3.924	431.311	588.618	352.658	134.412	16.412	−0.040	1411.934
$P = 0$ T (K)	a (Å)	B (GPa)	C_{11} (GPa)	C_{12} (GPa)	C_{44} (GPa)	$\tilde{C}_{44}$	$\tilde{C}_{11} - \lvert\tilde{C}_{12}\rvert$	$\tilde{C}_{11} + 2\lvert\tilde{C}_{12}\rvert$
0.000	4.718	68.081	182.734	10.754	49.144	49.144	171.981	204.242
150.000	4.721	67.372	181.907	10.105	48.509	48.509	171.802	202.117
300.000	4.739	65.395	179.222	8.482	47.468	47.468	170.740	196.186
450.000	4.766	60.294	171.819	4.531	43.294	43.294	167.287	180.881
600.000	4.799	54.643	163.640	0.145	39.158	39.158	163.494	163.930
750.000	4.839	49.079	156.165	−4.464	36.055	36.055	151.701	147.237
900.000	4.887	43.379	147.071	−8.466	30.694	30.694	138.604	130.138
1050.000	4.946	35.986	136.294	−14.169	23.729	23.729	122.125	107.957

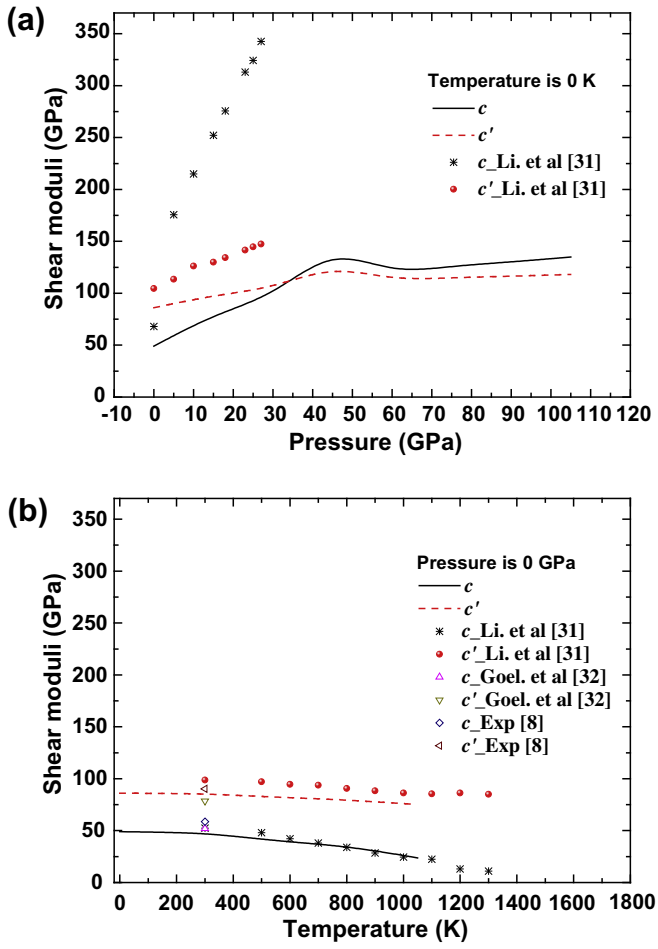

Fig. 2. c and c' of $^6Li_2O$ compared with other data of Li_2O at different temperature and pressure. (a) Temperature is 0 K and (b) pressure is 0 GPa.

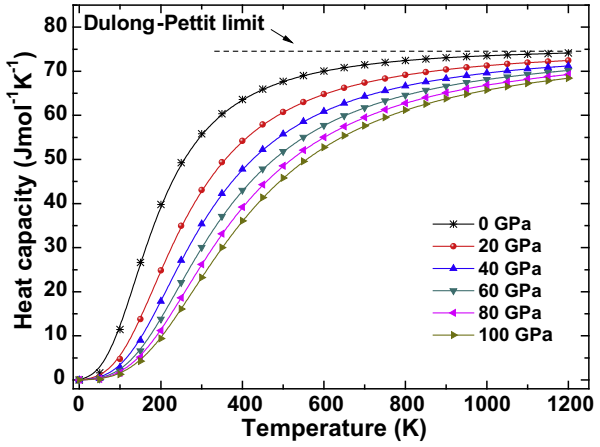

Fig. 3. The heat capacity vs temperature at pressure of 0–100 GPa.

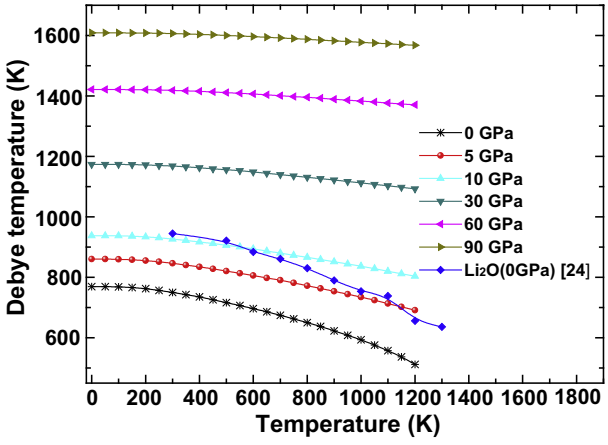

Fig. 4. The Debye temperature as a function of temperature at pressure of 0–90 GPa.

dependence of C_v is governed by the details of vibrations of the atoms. The sharp increase of $C_v(T)$ up to ~300 K is due to the anharmonic approximation of the Debye model. However, at higher temperature, the anharmonic effect on C_v is suppressed, and C_v is very close to the Dulong–Pettit limit, common to all solids at high temperatures. It can be seen from Figs. 3 and 4 that, with increasing temperature, C_v increases and θ decreases. However, as pressure

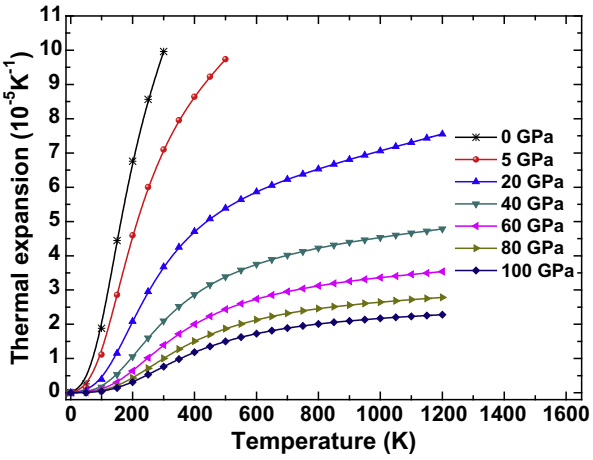

Fig. 5. The thermal expansion as a function of temperature at pressure of 0–100 GPa.

increases, C_v reduces and θ raises. Heat capacity C_v in this work is 55.8 J/mol · K at zero pressure and ambient temperature (300 K). Moreover, θ obtained here is 750.22 K. Compared with $^7Li_2O$, when pressure is 0 GPa, Debye temperatures of $^6Li_2O$ are lower (Fig. 4). Unfortunately, to our knowledge, there are no experimental or other theoretical data of C_v and θ of $^6Li_2O$ for our comparison.

Finally, in Fig. 5, we plot our results of the thermal expansion coefficient α of $^6Li_2O$. We remark that for a given pressure, α increases rapidly with temperature at low temperatures (<200 K) especially at zero or low pressure, and then increase slowly at higher temperatures gradually. As pressure increases, the increasing of α with temperature becomes smaller. While for a given temperature, α decreases rapidly with increasing pressure. As shown in Fig. 5, under low pressure, thermal expansion is obvious. However, with increasing pressure, thermal expansion is restrained obviously. The result is agreed with above.

4. Conclusions

In summary, in this work, the elastic and thermodynamic properties of *fcc*-$^6Li_2O$ under high temperatures and pressures are investigated using the Density functional theory and quasi-harmonic Debye model. Because of difference of zero-point energy of ^6Li and ^7Li, calculated lattice constant of $^6Li_2O$ at ground state is a little larger than that of $^7Li_2O$. Thermal expansion will be suppressed by pressure effectively. When temperature is 1200 K, just 8.59 GPa of pressure can keep the cell volume be V_0. Elastic constants indicate that crystal lattice of $^6Li_2O$ is mechanically stable at high temperature and pressure. Compared with Li_2O, shear of $^6Li_2O$ on the {1 0 0} and {1 1 0} planes caused by high pressure and temperature is lower. Heat capacity of different pressure increases with temperature and closes to the Dulong–Petit limit at higher temperatures. Debye temperature decreases with temperature, and increases with pressure. Furthermore, under lower pressure, thermal expansion coefficient raise rapidly with temperature, and the increasing trend will get slow at higher pressure and temperature.

Acknowledgements

The authors thank Prof. M.A. Blanco (Departamento de Química Físicay Analítica, Facultad de Química, Universidad de Oviedo, Oviedo, Spain) for valuable suggestions about *Ab initio* calculations and quasi-harmonic Debye model in the manuscript.

References

[1] Y. Oishi, Y. Kamei, M. Akiyama, T. Yanagi, J. Nucl. Mater. 87 (1979) 341.
[2] B.E. Lang, M.H. Donaldson, B.F. Woodfield, A. Burger, U.N. Roy, V. Lamberti, Z.W. Bell, J. Nucl. Mater. 347 (2005) 125–133.
[3] P. Demontis, R. LeSar, M.L. Klein, Phys. Rev. Lett. 60 (1988) 2284.
[4] P. Demontis, M.L. Klein, R. LeSar, Phys. Rev. B 40 (1989) 2716.
[5] A.F. Goncharov, V.V. Struzhkin, M.S. Somayazulu, R.J. Hemley, H.K. Mao, Science 273 (1996) 218.
[6] P. Loubeyre, R. LeToullec, E. Wolanin, M. Hanfland, D. Hausermann, Nature (London) 397 (1999) 503.
[7] C. Cavazzoni, G.L. Chiarotti, S. Scandolo, E. Tosatti, M. Bernasconi, M. Parrinello, Science 283 (1999) 44.
[8] S. Hull, T.W.D. Farley, W. Hayes, M.T. Hutchings, J. Nucl. Mater. 160 (1988) 125.
[9] Y.Y. Liu, M.C. Billone, A.K. Fischer, S.W. Tam, R.G. Clemmer, Fusion Technol. 8 (1985) 1970.
[10] L. Fast, J.M. Wills, B. Johansson, O. Eriksson, Phys. Rev. B 51 (1995) 17431.
[11] G.V. Sin'ko, N.A. Smirnow, J. Phys.: Condens. Matter. 14 (2002) 6989.
[12] M.A. Blanco, E. Francisco, V. Luaña, Comput. Phys. Commun. 158 (2004) 57–72.
[13] W.Y. Ren, P.C. Xu, W.G. Sun, Physica B 405 (2010) 2057–2060.
[14] F. Wang, W.D. Wu, Y.J. Tang, Acta Phys. Sinica 59 (5) (2010) 663–668.
[15] J.P. Perdew, K. Burke, M. Ernzerhof, Phys. Rev. Lett. 77 (1996) 3865.
[16] B. Hammer, L.B. Hansen, J.K. Norskov, Phys. Rev. B 59 (1999) 7413.
[17] M.A. Blanco, A. Martín Pendás, E. Francisco, J.M. Recio, R. Franco, J. Molec. Struct. Theochem. 368 (1996) 245.
[18] M. Flórez, J.M. Recio, E. Francisco, M.A. Blanco, A. Martín Pendás, Phys. Rev. B 66 (2002) 144112.
[19] E. Francisco, J.M. Recio, M.A. Blanco, A. Martín Pendás, A. Costales, J. Phys. Chem. 102 (1998) 1595.
[20] J.P. Poirier, Introduction to the Physics of the Earth's Interior, vol. 39, Cambridge University Press, Oxford., 2000.
[21] R. Hill, Proc. Phys. Soc. London A 65 (1952) 349.
[22] F.D. Murnaghan, Proc. Natl. Acad. Sci. USA 30 (1944) 5390.
[23] R. Dovesi, C. Roetti, C. Freyria-Fava, M. Prencipe, Chem. Phys. 156 (1991) 11.
[24] J. García Rodeja, M. Meyer, M. Hayoun, Modelling Simul. Mater. Sci. Eng. 9 (2001) 81.
[25] M. Wilson, S. Jahn, P.A. Madden, J. Phys.: Condens. Matter. 16 (2004) S2795.
[26] S. Hull, T.W.D. Farley, W. Hayes, M.T. Hutchings, J. Nucl. Mater. 160 (1988) 125.
[27] B. Johansson, A. Rosengren, J. Phys. F: Metal Phys. 5 (1975) L15–L17.
[28] E.J. Covington, D.J. Montgomery, J. Chem. Phys. 27 (1957) 1030.
[29] W.Y. Ren, F. Wang, P.C. Xu, W.G. Sun, European Physical: J. Appl. Phys. in press.
[30] C. Kittel, Introduction to Solid State Physics, eighth ed., John Wiley and Sons (WIE), US, 2004.
[31] X.F. Li, X.R. Chen, Solid State Commun. 139 (2006) 197–200.
[32] P. Goel, N. Choudhury, S.L. Chaplot, Phys. Rev. B 70 (2004) 174307.
[33] A. Einstein, Ann. Phys. 22 (1907) 180.
[34] W. Nernst, A.F. Lindemann, Z. Elektrochem. Angew. Phys. Chem. 17 (1977) 817.
[35] P. Debye, Ann. Phys. 39 (1912) 789.
[36] A.T. Petit, P.L. Dulong, Ann. Chim. Phys. 10 (1819) 395.